ResearchGate

See discussions, stats, and author profiles for this publication at: https://www.researchgate.net/publication/321123868

When water meets iron at Earth's core mantle boundary

Article *in* National Science Review · September 2017

DOI: 10.1093/nsr/nwx109

CITATIONS
115

READS
1,315

10 authors, including:

Qingyang Hu
Center for High Pressure Science & Technology Advanced Research
114 PUBLICATIONS **3,821** CITATIONS

SEE PROFILE

Liuxiang Yang
Carnegie Institution for Science
98 PUBLICATIONS **4,657** CITATIONS

SEE PROFILE

Jin Liu
HPSTAR
77 PUBLICATIONS **3,218** CITATIONS

SEE PROFILE

All content following this page was uploaded by Qingyang Hu on 10 December 2017.

The user has requested enhancement of the downloaded file.

RESEARCH ARTICLE

National Science Review
0: 1–9, 2017
doi: 10.1093/nsr/nwx109
Advance access publication 8 September 2017

GEOSCIENCES

When water meets iron at Earth's core–mantle boundary

Ho-Kwang Mao[1,2,*,†], Qingyang Hu[1,2,3,†], Liuxiang Yang[1,2,†], Jin Liu[3], Duck Young Kim[1], Yue Meng[4], Li Zhang[1], Vitali B. Prakapenka[5], Wenge Yang[1] and Wendy L. Mao[3]

ABSTRACT

Hydrous minerals in subducted crust can transport large amounts of water into Earth's deep mantle. Our laboratory experiments revealed the surprising pressure-induced chemistry that, when water meets iron at the core–mantle boundary, they react to form an interlayer with an extremely oxygen-rich form of iron, iron dioxide, together with iron hydride. Hydrogen in the layer will escape upon further heating and rise to the crust, sustaining the water cycle. With water supplied by the subducting slabs meeting the nearly inexhaustible iron source in the core, an oxygen-rich layer would cumulate and thicken, leading to major global consequences in our planet. The seismic signature of the D″ layer may echo the chemical complexity of this layer. Over the course of geological time, the enormous oxygen reservoir accumulating between the mantle and core may have eventually reached a critical eruption point. Very large-scale oxygen eruptions could possibly cause major activities in the mantle convection and leave evidence such as the rifting of supercontinents and the Great Oxidation Event.

Keywords: high pressure, core–mantle boundary, water and iron

[1]Center for High Pressure Science and Technology Advanced Research, Shanghai 201203, China; [2]Geophysical Laboratory, Carnegie Institution, Washington, DC 20015, USA; [3]Department of Geological Sciences, Stanford University, Stanford, CA 94305, USA; [4]High Pressure Collaborative Access Team (HPCAT), Geophysical Laboratory, Carnegie Institution, Argonne, IL 60439, USA and [5]Center for Advanced Radiation Sources, University of Chicago, Chicago, IL 60437, USA

*Corresponding author. E-mail: hmao@gl.ciw.edu
†Equally contributed to this work.

Received 11 July 2017; **Revised** 9 August 2017; **Accepted** 25 August 2017

INTRODUCTION

Among all of the global boundaries on the planet, the interface between Earth's core and mantle stands out as having the greatest contrast in chemical composition and physical properties [1]. The enigmatic signature from seismic observations of the D″ layer on top of the core–mantle boundary (CMB) [2] has long eluded satisfactory explanation. Our recent high-pressure-temperature (*P-T*) studies revealed that a newly discovered iron hydrodioxide (FeO_2Hx, designated as the Py-phase and $0 < x < 1$) with cubic $Pa\bar{3}$ space group symmetry and the pyrite structure [3,4] could be a candidate mineral for the D″ layer. While we worked on the revision of this manuscript, Nishi *et al.* also confirmed the formation of the pyrite-type phase of FeOOH [5]. They suggested that goethite sandwiched in layers of SiO_2 would transform into the pyrite-type high-pressure phase without loss of any hydrogen at conditions below 2400 K at 111 GPa and 1500 K at 129 GPa. These studies also exemplify the drastic changes of chemistry occurring on the most basic elements under the *P-T* conditions of the deep lower mantle. In the present work, we conducted additional experiments in the key Fe-O-H ternary system, presented the mechanism for generating widespread oxygen-rich patches consisting of the Py-phase and other iron oxides and hydrides at the base of the mantle, and proposed far-reaching geophysical, geochemical and geodynamic consequences based on the new observations.

The Py-phase was previously synthesized at the *P-T* conditions of the deep lower mantle (DLM >1800-km depth) by oxidizing hematite (Fe_2O_3) or dehydrogenating goethite (FeO_2H) [3]. However, neither hematite nor goethite is a major mineral in the crust; their abundances are insufficient to form a significant portion of the D″, which is more massive than the entire crust. Searching for a possible source of much greater magnitude, we found that, if hydrous minerals go down with slabs to reach the subsolidus side of CMB [6–10], the nearly inexhaustible iron reservoir in the core will react with the water released from the hydrous minerals to generate an enormous quantity of the Py-phase in oxygen-rich patches (ORP) above the CMB. The formation

© The Author(s) 2017. Published by Oxford University Press on behalf of China Science Publishing & Media Ltd. All rights reserved. For permissions, please e-mail: journals.permissions@oup.com

Downloaded from https://academic.oup.com/nsr/advance-article-abstract/doi/10.1093/nsr/nwx109/4107791
by guest
on 10 December 2017

of the ORP leads to a range of extremely important consequences and implications including: the source of seismic complexity in the D″ layer [2], the chemical and geodynamic metastability of the ORP, the Great Oxidation Event [11] and the episodic dispersions of supercontinents [12].

RESULTS

When water meets iron at moderate *P-T* above 5 GPa, it oxidizes and hydrogenates iron to form wüstite and iron hydride [13,14], namely

$$3Fe + H_2O = FeO\ (\text{wüstite}) + 2FeH. \quad (1)$$

For simplification, here we refer to wüstite Fe_xO with $x = 0.9–0.947$ as FeO, and FeH_x with $x \leq 1$ as FeH. The simplification does not affect our discussion and conclusion. The assemblage FeO + FeH can coexist with excess water or iron under moderate pressures.

We conducted the same experiment at high *P-T* corresponding to DLM conditions, and observed a dramatically different pressure-induced chemistry that made H_2O a much more powerful oxidizer. We suspended a piece of iron foil in excess H_2O in a Re gasket, which was compressed in a diamond-anvil cell (DAC) up to 96 GPa and heated with infrared lasers to 2200 K. As shown in the x-ray diffraction (XRD) pattern (Fig. 1), the oxidation product went far beyond wüstite, passing across the entire oxidation series of iron oxides to the most oxygen-rich dioxide (Py-phase) FeO_2H_x with $x \leq 0.73$ (see the 'Methods' section and Supplementary Table 1, available as Supplementary Data at *NSR* online), plus FeH:

$$4Fe + 2H_2O = FeO_2H_x\ (\text{Py-phase}) + 3FeH. \quad (2)$$

Again, for simplicity, we neglect the non-stoichiometry of FeH and the hydrogen loss $(1 - x)$H in the equation.

We also experimented with water reacting with hematite Fe_2O_3, which was previously known as the most oxidized form of iron oxides. Water oxidizes hematite further to form the Py-phase at 110 GPa and 2250 K (Fig. 2):

$$Fe_2O_3 + H_2O = 2FeO_2H_x\ (\text{Py-phase}). \quad (3)$$

Reactions (2) and (3) bracket the entire iron oxide series from Fe, FeO, Fe_3O_4 to Fe_2O_3, including the newly discovered Fe_5O_6 [15], Fe_4O_5 [16], Fe_5O_7 and $Fe_{25}O_{32}$ [17]; every phase within the bracket must react with H_2O to produce the same assemblage of the Py-phase and FeH. Indeed, our experiments confirmed the following reactions (Supplementary Fig. 1 and Supplementary Table 1, available as Supplementary Data at *NSR* online):

$$4FeO + 2H_2O = 3FeO_2H_x\ (\text{Py-phase}) + FeH \quad (4)$$

and

$$4Fe_3O_4 + 6H_2O = 11FeO_2H_x\ (\text{Py-phase}) + FeH. \quad (5)$$

These reactions can be illustrated by the Fe-O-H ternary phase diagram for DLM conditions (Fig. 3).

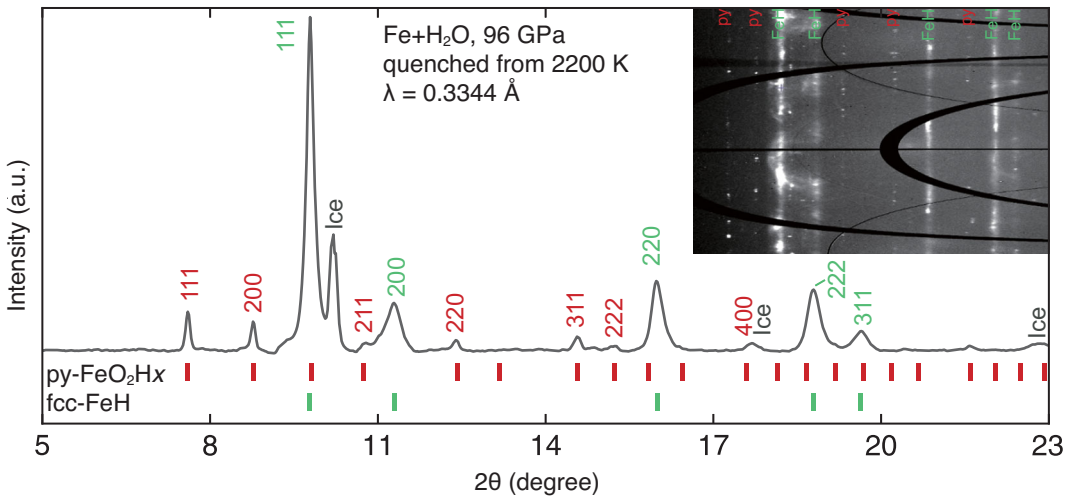

Figure 1. XRD pattern of reaction products of iron and water. Iron powder was compressed in H_2O to 96 GPa, heated up to 2200 K for 5 minutes, and quenched to 300 K. The pattern was composed of the Py-phase ($a = 4.370(3)$ Å), the quenchable high-temperature f.c.c. phase [44] of FeH ($a = 3.397(4)$ Å) and excess ice VII. Inset figure is the caked diffraction pattern, showing the coexistence of the Py-phase (dotted reflections) and FeH (continuous reflections).

Downloaded from https://academic.oup.com/nsr/advance-article-abstract/doi/10.1093/nsr/nwx109/4107791
by guest
on 10 December 2017

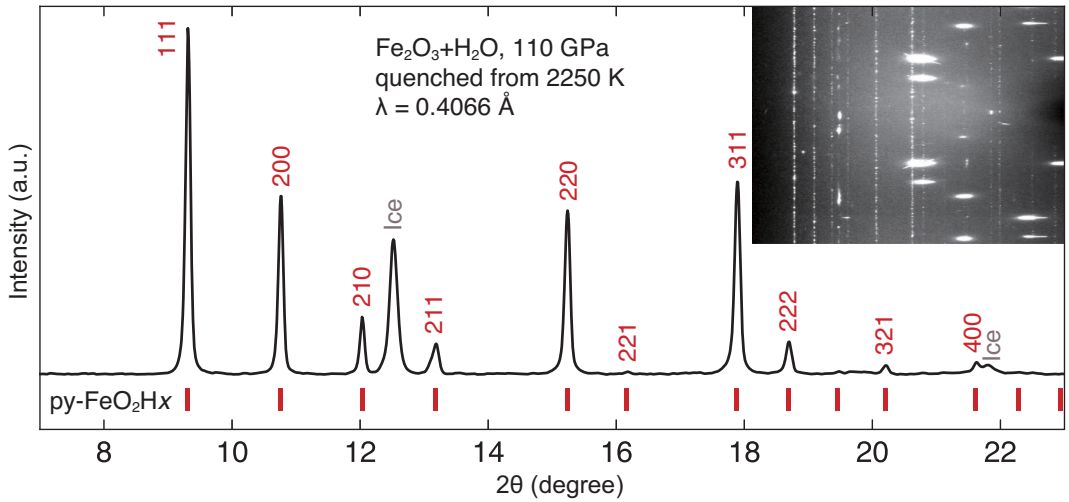

Figure 2. XRD pattern of reaction product of Fe_2O_3 and water. The sample was compressed to 110 GPa, heated to 2250 K and quenched to 300 K. py, pyrite structured FeO_2Hx. Inset figure is the caked image with dotted Py-phase reflections, scattered ice spots and bright diamond spots.

With the starting compositions of Fe, FeO, Fe_3O_4 or Fe_2O_3 in H_2O (light blue lines), the final products all fall within the FeO_2H_x (Py-phase)-FeH-H_2O three-phase triangle, as shown in Equations (2)–(5). Because iron is the most abundant element on Earth by mass, oxygen is the most abundant element by number of atoms and hydrogen is the most mobile element, this ternary provides an essential view of our planet. Normally, when we considered the mantle and core as separate entities, the focus on the mantle would be on the multicomponent system of Si, Mg, Al, Ca oxides, with Fe as one of the elements, and the focus of the core would be on the Fe alloy system, with O and H as minor components among Si, S, C, etc. However, when Reactions (2)–(5) are allowed to proceed extensively to generate a massive layer at the CMB, the Fe-O-H ternary and the reaction layer must take a dominant role and dictate first-order Earth processes.

IMPLICATIONS OF IRON–WATER REACTIONS AT THE CMB

Reactions (2)–(5) can certainly occur, but how prevalent are these reactions at the CMB? The amount of the Py-phase produced at the CMB depends upon the available H_2O. An ever–growing number of high-*P* hydrous minerals have been discovered and recently reported [6–10]. It is reasonable to assume that some of these hydrous phases can be transported down to the CMB through plate tectonic processes. The sharply rising temperature ($\Delta T \sim 1000$ K) [18] near the core will dehydrate the minerals and release water. As we observed in experiments, the water would then react with iron on the subsolidus side of the CMB to form a veneer of iron dioxide and hydride according to reaction (2). Iron and iron dioxide are two extreme end members of the oxidation-reduction series; between them, the full stoichiometric series of intermediate layers must form (Fig. 3, top thick blue bar). Local chemical equilibria are maintained throughout the cascading stoichiometry of the multilayers. The growth process of the multilayers via diffusion and infiltration in a chemical gradient is very similar to the bimetasomatism in metamorphic petrology [19,20], except on a much more widespread, global scale.

With the unlimited supply of iron from the core and oxygen from the mantle, and a relatively small amount of hydrogen in the Earth, sustaining the growth of the ORP relies on recycling of hydrogen. According to Reactions (2)–(5), while H_2O causes oxidation of iron to dioxide, it also causes hydrogenation of iron to FeH_x hydride. However, the hydrogen will not be trapped like oxygen, but will most likely escape and continue its circulation. A large amount of hydrogen escaped at the initial reaction stage as the missing balance of the Reactions (2)–(5). The ORP moving laterally into hotter regions [18] would cause continuous hydrogen release because FeH melts at ~1000 K lower temperature [21,22] than major lower-mantle silicates and oxides and because the dissolved hydrogen in the FeO_2H_x Py-phase decreases with increasing *T* and prolonged heating (see 'Methods' section). The hydrogen loss pushes the overall composition of the ORP toward the Fe-O axis of the ternary diagram, as shown by large downward arrows and the bottom shaded area (Fig. 3).

Downloaded from https://academic.oup.com/nsr/advance-article-abstract/doi/10.1093/nsr/nwx109/4107791
by guest
on 10 December 2017

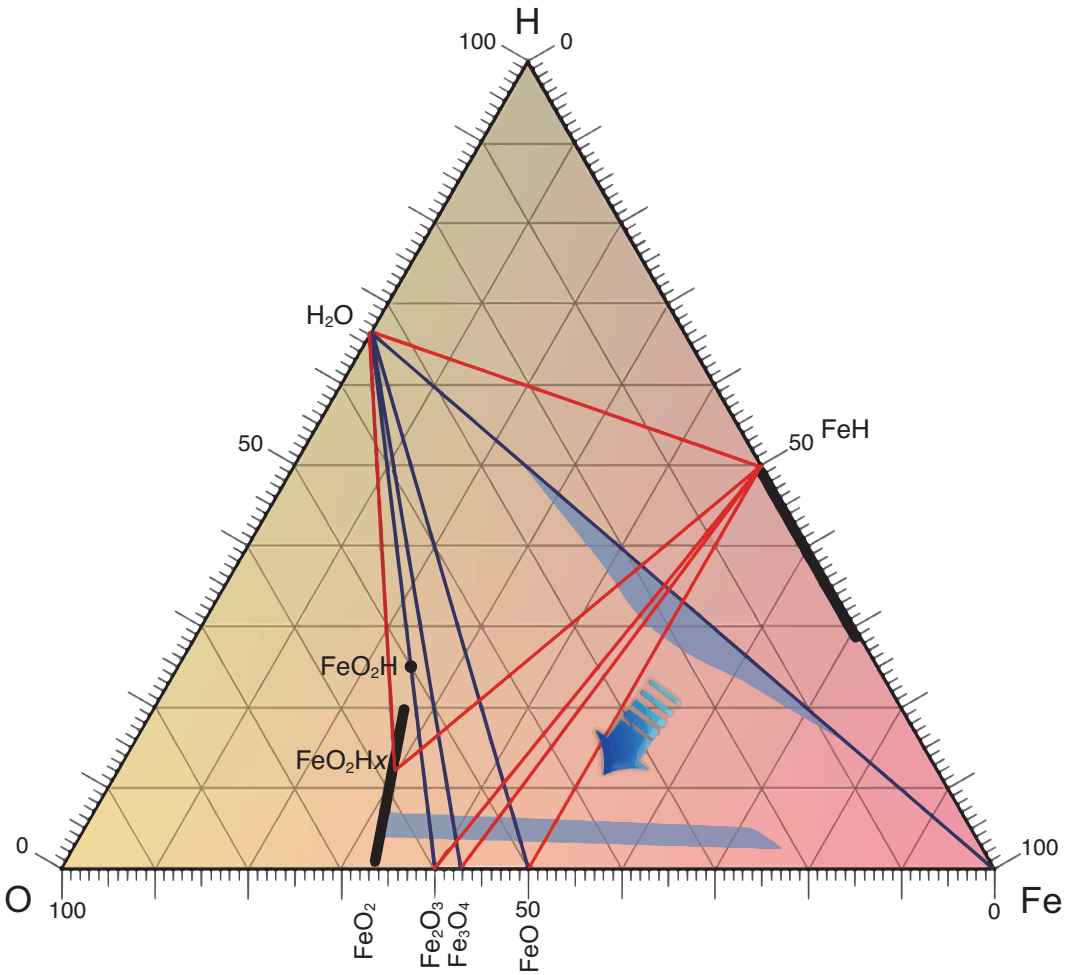

Figure 3. Fe-O-H ternary phase diagram (atomic %) under DLM *P-T* conditions. Two-phase tie lines are shown in red. To avoid cluttering, Fe_5O_6 [15], Fe_4O_5 [16], Fe_5O_7 and $Fe_{25}O_{32}$ [17] are not plotted. The compositional ranges of the Py-phase and iron hydride are shown as black bars. To avoid over-cluttering the diagram, only one tie line is drawn through each phase with variable compositions. The blue lines represent Reactions (2)–(5). The top thick blue shade represents the composition of the reaction multilayer when water meets the iron core. With the loss of hydrogen, the composition shifts along the direction of the arrow toward the bottom shaded area.

The escaped hydrogen is light and mobile. It may infiltrate through the grain boundaries of mantle minerals or form other volatiles, such as hydrocarbons, that ascend to Earth's surface through the mantle, thus completing the hydrogen cycle and leaving behind the ORP. The net result of the hydrogen cycle, therefore, works like an oxygen pump that transports and delivers oxygen to the CMB.

An alternative hypothesis assumed that the liquid outer core was undersaturated with hydrogen, then the liquid core would dissolve and absorb all hydrogen [6]. We do not consider this a viable hypothesis. The only available data on hydrogen solubility came from Okuchi's experimental study [21,22] of hydrogen in molten iron at pressures below 7.5 GPa, which is not a plausible constraint for the CMB condition at 130 GPa in view of the drastic change of iron chemistry under pressure. In addition, if a significant fraction of the hydrogen cycle ended as a one-way journey to the core, the hydrosphere would be long gone and the Earth's surface would be as dry as that of Mars.

Hydrous minerals bring the water down continuously and endlessly, adding oxygen to ORP throughout the 4.5-Ga lifetime of the Earth. The rate at which water enters into subduction zones has been estimated to be at around 1×10^{12} kg/year of water [23,24]. A new estimation [25] predicted most water would return to the surface through arc volcanism and only 30% would go down to the deep mantle. The total budget of the Py-phase that could be generated would be equivalent to a 4-km-thick shell covering the entire CMB. However, the Py-phase is only one component among oxides of the ORP, and including FeH*x* and other iron oxides in the reaction series will increase the thickness of ORP

Downloaded from https://academic.oup.com/nsr/advance-article-abstract/doi/10.1093/nsr/nwx109/4107791
by guest
on 10 December 2017

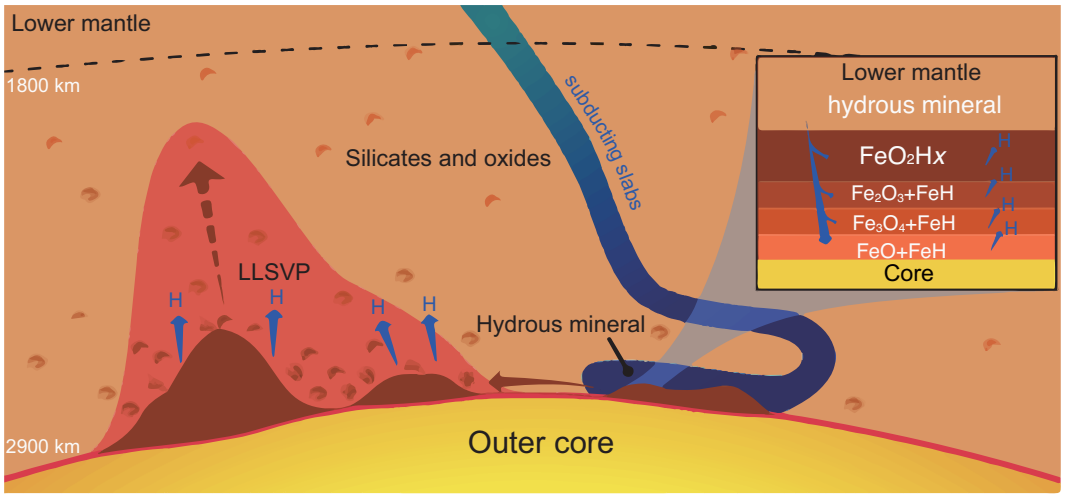

Figure 4. Schematic diagram of ORP in the DLM. Hydrous minerals in the subducting slab (blue) carry H_2O to react with the iron core to form the ORP (dark brown) which is a multilayer with increasing oxygen content (inset). H_2O penetrates the multilayer to produce more Py-phase, and hydrogen escapes from FeH and FeO_2Hx and ascends upwards to sustain the hydrogen cycle. The ORP moves laterally and accumulates. Some ORP (small patches) are scattered and mixed with the DLM silicates and oxides.

substantially. Moreover, spatial distribution in ORP are expected to be very uneven (Fig. 4) and some regions can be much thicker.

The density of the Py-phase (7.0∼7.6 g/cm^3, estimated at 3000 K) and iron oxide series [26] are considerably higher than the average silicate mantle (∼5.5 g/cm^3) but lower than the liquid iron (∼10 g/cm^3) at the CMB [27]. The ORP will float between the core and mantle, and only move laterally from its point of generation at the cooler down-going slab to hotter regions [18] following the whole mantle convection. Due to the density contrast, it will not rise with the plume, but will reside and grow indefinitely. Analogous to the isostasy of continental crust on the mantle, the bottom of a very thick ORP would dip into the outer core (Fig. 4).

With the ORP as a potentially important component in addition to the silicates in the D″ layer, we can now address many of its complexities [2]. The ORP will originate in regions where the wet, down-going slab meets the core, float on the CMB and accrete as a result of continuous mantle convection. Its distribution will be highly uneven at the global scale. The reaction lamella of the multilayers may lead to shape preferred orientation, causing the observed shear wave splitting in the D″ layer. Based on Birch's Law [28], which correlates mean atomic number and acoustic velocity, the iron oxides with high mean atomic numbers would have considerably lower compressional velocity compared to the surrounding silicate mantle. Iron oxides alone or their mixtures with mantle silicates may account for the low velocities found in large low shear velocity provinces (LLSVP) and ultra-low velocity zones (ULVZ)—two characteristic features in the DLM. In fact, ULVZ may predominantly consist of ORP. Various iron oxides, hydride, their possible phase transitions and different mixtures with silicates provide a set of rich, adjustable parameters to answer all unusual seismic features, including the anti-correlation of the compressional and shear velocities and the large lateral variability in the D″ layer. Quantitative analyses, however, await direct mineral physical studies of velocities of the ORP and its constituents as a function of P, T and x.

IMPLICATIONS OF ORP TO GLOBAL EVENTS

If a substantial amount of ORP cumulates at the CMB, it will dramatically change the conventional views of the global geochemistry; its impact cannot be overlooked. Now we would like to consider the long-term stability of ORP at the CMB and postulate its full consequences. For a fixed composition between Fe and H_2O (Fig. 3), the phase rule of a fully equilibrated three-component close system can only have one of the four three-phase assemblages: Fe-FeO-FeH, FeO-Fe_3O_4-FeH, Fe_3O_4-Fe_2O_3-FeH or Fe_2O_3-FeO_2Hx-FeH. However, for an open system of a chemical gradient between two infinite sources of Fe and H_2O, a bimetasomatic zoning sequence of Fe-FeO-FeH, FeO-Fe_3O_4-FeH, Fe_3O_4-Fe_2O_3-FeH or Fe_2O_3-FeO_2Hx-FeH will grow in between the two end members. On the local scale, the ORP would have maintained local equilibrium at each point of the chemical gradient between the

Downloaded from https://academic.oup.com/nsr/advance-article-abstract/doi/10.1093/nsr/nwx109/4107791
by guest
on 10 December 2017

Py-phase and Fe core. A chemically stable bimetasomatic steady state will be dictated by diffusion and infiltration [19,20] (Fig. 3). The iron oxides and hydride are considerably denser than the overlaying silicate mantle but lighter than the underneath iron core. Within the multilayers, the density profile also increases downward with increasing Fe/O ratio. Therefore, the ORP is chemically and gravitationally stable and can keep growing indefinitely without disturbance.

On the overall global scale, however, the system is only metastable. After releasing hydrogen, with the extremely oxidized ORP sandwiched in between the highly reducing lower mantle [29] and the even more reducing core, the large quantity of excess oxygen is poised for catastrophe to happen. For instance, with major perturbations that move the CMB thermal boundary layer [18] up by several hundred degrees, the ORP would partially melt and release its excess oxygen:

$$2FeO_2Hx = Fe_2O_3 + xH_2O + {}^1\!/\!_2\,(1-x)\,O_2. \quad (6)$$

The high-temperature decomposition to Fe_2O_3 was also observed in Ref. [5] and in our preliminary experiments, although the exact temperature is not well constrained. Reference [5] postulates an isochemical transition from ε-FeO_2H to Py-FeO_2H that implies $x = 1$ and no O_2. However, the isochemical assumption is in direct contradiction with their own report of excess FeH which mandates change of chemistry. For $x \ll 1$ [4], the released material will be essentially oxygen. The oxygen may rise as O_2 or react to form other volatiles, such as CO, CO_2, H_2O, SO_2 and NO_2, thus reducing the viscosity and accelerating the plume uprising. A small-scale oxygen release would be uneventful and unnoticeable as a part of regular mantle convection. A large-scale oxygen eruption in ORP, however, could cause geodynamic instability and mantle overturn analogous to the limnic eruption of oversaturated dissolved CO_2 causing runaway lake overturn [30], except the solid mantle is on a much larger scale and longer process than the fluid lake water. The perturbation could come from a variety of sources ranging from the steady growth of the ORP that reached a critical isostasy overload that bends the CMB to cross the thermal boundary to a sudden impact by an astronomical object that could also shift the thermal boundary layer and cause a runaway oxygen eruption.

We further hypothesize that initially Earth may have taken its first 2 Ga to accumulate multiple ORPs from scratch to a supersaturated, critical state and an oxygen eruption was then triggered by further overloading or asteroid impact. The corresponding geodynamic instability could also be responsible for the breakup of the Kenorland supercontinent [31]. After the first major outburst releasing overabundant oxygen, the ORP would drop back to a 'normal' undersaturated condition, but still hold an excess quantity of oxygen. It would not need to accumulate from scratch, and the critical overloading would take shorter time intervals to reach. The number of subsequent eruptions would be more frequent but smaller, corresponding to the half-dozen episodic supercontinent breakups in the past 2.5 Ga of geological history [12,32].

Direct geological evidence for ORP eruption would be a sudden rise in the oxygen level on the surface. The Great Oxidation Event (GOE) [11], which occurred approximately concurrently with the Kenorland breakup, fits the bill. Earth's atmosphere, originally deprived of oxygen, was suddenly filled with oxygen, and the explosion of aerobic life followed. The process is similar to CO_2 eruption in oversaturated lakes, except limnic eruption destroys lives [30], but the GOE eruption created lives, as we know. Indirect evidence may include the widespread banded-iron formation that was formed through a sedimentary process in iron-rich sea water [26,31]. Other indirect evidence of a sudden increase in atmospheric oxygen may include the environmental changes that led to snowball Earth and five mass extinctions.

CONCLUSION

In summary, our experiments and calculations show a surprisingly different pressure-induced chemistry between Fe and H_2O at the DLM conditions. We demonstrate that, when sufficient water meets the iron core over extended geological time, a Py-phase-bearing oxygen-rich layer must cumulate at the CMB. The consequence of the ORP would lead to great impacts on our fundamental notions of deep Earth and its history, including the origins of the D″ layer, the core–mantle geochemistry, the GOE and the super activities of plate tectonics. A new set of working hypotheses is emerging based on the logical extension of our new experimental evidence in the Fe-O-H system. A new set of research efforts is needed to provide the critical tests.

METHODS

Angular dispersive XRD experiments

Angular dispersive XRD experiments were performed at 13-IDD of GeoSoilEnviroCARS

Downloaded from https://academic.oup.com/nsr/advance-article-abstract/doi/10.1093/nsr/nwx109/4107791
by guest
on 10 December 2017

(GSECARS) and 16ID-B/16BM-D of HPCAT, Advanced Phonon Source (APS), Argonne National Laboratory (ANL). Iron (Sigma-Aldrich CAS: 7439-89-6) or iron oxide samples of wüstite (Alfa Aesar CAS: 1345-25-1), magnetite (Alfa Aesar CAS: 1317-21-9) and hematite (American Elements FE-OX-57-ISO) are commercially available. Only hematite was annealed at 1000°C for 24 h. All samples were pre-compressed to ∼10-μm thickness and a size of ∼20 × 20 μm^2 before loading into DAC. High pressure was achieved by using diamond anvils with 100- or 150-μm culet diameter (beveled from 300 μm) and with a hole of 34 μm (for 100-μm culets) or 52 μm (for 150-μm culets) in diameter in rhenium gaskets. De-ionized water served as the pressure medium as well as the thermal insulator. Ruby balls and a small gold chip were placed near the sample for pressure calibration. The uncertainty in pressure is as large as 0.5 GPa equivalent to the minimum step to index gold equation of state (EOS) [33]. For those experiments that had no gold chips, the EOS of ice and diamond Raman edge was used for measureing pressure (Supplementary Table 1, available as Supplementary Data at *NSR* online) [34]. Samples were heated at 13ID-D of GSECARS [35], 16ID-B of HPCAT [36] and offline at High Pressure Synergetic Consortium (HPSynC) at APS. Heating temperatures were measured by fitting the black-body radiation curves on both sides. The diameter of the laser spot is estimated at around 20 μm (estimated by spot diameter) at 2000 K at HPCAT. Laser spots at GSECARS and HPSynC are approximately 15 μm in diameter at 2000 K.

First principles simulations

EOS curves of FeO_2 and FeO_2H were calculated using Density Functional Theory plus the on-site Coulomb interaction U (DFT+U) approach implemented in the VASP software package [37]. Our simulation focuses on the accuracy of structural parameters. In light of this, we used small core pseudo potentials for O and H, and a standard potential for Fe within the Generalized Gradient Approximation (GGA) [38] of Perdew, Burke, Ernzerhof (PBE) [39] for the exchange correlation description. The plane-wave cutoff is set to 1000 eV and the Brillouin zone sampling was performed with a uniform grid sampling of 16 × 16 × 16. To describe localized d-orbital electrons of Fe properly, we used DFT+U [40] with a rotational invariant. In our previous theoretical study [41], we investigated an optimal value set of U (on-site Coulomb interaction) = 5 eV and J = 0.8 eV (Hund coupling constant) for FeO_2. While the Fe-O bonding in the Py-phase is not sensitive to the choice of U and J, those parameters strongly influence the length of O-O dimer in the Py-phase lattice. Following the prescription above, the calculated structure is able to reproduce the experimental O-O bonding length in FeO_2 (e.g. ∼1.9 Å at 75 GPa) with slightly smaller bulk volume (e.g. ∼2% smaller than the experiment at 75 GPa). The same set of parameters is used for FeO_2H. As DFT+U calculations are conducted at zero temperature and to consider thermal expansion of volume at 2500 K to the volume–pressure relations, we also employed a quasi-harmonic approximation introduced in the Phonopy software [42].

Determination of hydrogen in the Py-phase

First principles calculations show that, at 0 K and high pressures, FeO_2 and FeO_2H have the identical pyrite structure with cubic $Pa\bar{3}$ space group symmetry; the only difference is that FeO_2H has a larger unit-cell volume than FeO_2, corresponding to the additional H. In high-P-T syntheses, we found that they form a complete solid solution (the Py-phase, FeO_2Hx) with a linear unit-cell volume *vs.* x relation [4]. Increasing temperature and prolonged heating can both reduce x. Even with the lowest synthesis temperatures and short heating time, we still observed hydrogen loss in FeO_2Hx, [43] indicating $x < 1.0$. The hydrogen loss is demonstrated in stoichiometric starting goethite FeO_2H by the detection of escaped H_2 in Ne pressure medium or observation of initial growth of FeH.

For calibration of the V–x relations, we have the firm baseline of $x = 0$ from pure FeO_2 synthesized in an O_2 environment free of H. Without the x = 1 point, we adopt the volume percentage difference between FeO_2 and FeO_2H, which is more accurate than the absolute volume prediction from theory alone. We use the relation:

$$x = \frac{V - V_0}{V_{c1} - V_{c0}}, \tag{7}$$

where V, V_0, Vc_1 and Vc_0 are the volume of the FeO_2Hx determined in experiment, the volume of FeO_2 from the experimental EOS, the volume for x = 1 (FeO_2H) from simulation and the volume for x = 0 (FeO_2) from simulation, respectively, at the same P and 300 K. Based on this relation, we estimate that the maximum amount of hydrogen that the Py-phase FeO_2Hx can accommodate is x = 0.81 from the starting material of goethite, and the Py-phase that we synthesized in H_2O-saturated environment is

Downloaded from https://academic.oup.com/nsr/advance-article-abstract/doi/10.1093/nsr/nwx109/4107791
by guest
on 10 December 2017

$x = 0.45–0.73$ (Supplementary Table 1, available as Supplementary Data at *NSR* online).

SUPPLEMENTARY DATA

Supplementary data are available at *NSR* online.

ACKNOWLEDGEMENTS

We thank Q. Williams for valuable comments. We acknowledge S. Sinogeikin and J. Smith for beamline technical support. X-ray diffraction measurements were performed at High Pressure Collaborative Access Team (HPCAT, 16ID-B and 16BM-D) and GeoSoilEnviroCARS (GSECARS, 13ID-D), Advanced Photon Source (APS), Argonne National Laboratory.

FUNDING

This work is supported by the National Natural Science Foundation of China (U1530402). HPCAT operations are supported by the US Department of Energy (DOE)—National Nuclear Security Administration (NNSA) under award No. DE-NA0001974 and DOE—Basic Energy Sciences (BES) under award No. DE-FG02-99ER45775, with partial instrumentation funding by US National Science Foundation (NSF). GSECARS is supported by the NSF Earth Sciences (EAR-1634415) and DOE GeoSciences (DE-FG02-94ER14466). This research used resources of the APS, a DOE Office of Science User Facility operated for the DOE Office of Science by ANL under Contract No. DE-AC02-06CH11357. H.K.M., Q.H. and L.Y. were supported by NSF Geophysics Grant EAR-1345112 and Geochemistry Grant EAR-1447438. W.L.M., Q.H. and J.L. acknowledge support from NSF Geophysics Grant EAR-1446969.

REFERENCES

1. Hernlund JW and McNamara AK. The core–mantle boundary region. In: Schubert G (ed.). *Treatise on Geophysics*. Oxford, England: Elsevier, 2015, 461–519.
2. Lay T, Williams Q and Garnero EJ. The core-mantle boundary layer and deep Earth dynamics. *Nature* 1998; **392**: 461–8.
3. Hu Q, Kim DY and Yang W *et al*. FeO_2 and FeOOH under deep lower-mantle conditions and Earth's oxygen-hydrogen cycles. *Nature* 2016; **534**: 241–4.
4. Hu Q, Kim DY and Liu J. Dehydrogenation of goethite in Earth's deep lower mantle. *Proc Nat Acad Sci U S A* 2017; **114**: 1498–501.
5. Nishi M, Kuwayama Y and Tsuchiya J *et al*. The pyrite-type high-pressure form of FeOOH. *Nature* 2017; **547**: 205–8.
6. Walter MJ, Thomson AR and Wang W *et al*. The stability of hydrous silicates in Earth's lower mantle: experimental constraints from the systems MgO-SiO_2-H_2O and MgO-Al_2O_3-SiO_2-H_2O. *Chemical Geology* 2015; **418**: 16–29.
7. Nishi M, Irifune T and Tsuchiya J *et al*. Stability of hydrous silicate at high pressures and water transport to the deep lower mantle. *Nature Geosci* 2014; **7**: 224–7.
8. Shieh SR, Duffy TS and Liu Z *et al*. High-pressure infrared spectroscopy of the dense hydrous magnesium silicates phase D and phase E. *Phys Earth Planet In* 2009; **175**: 106–14.
9. Pamato MG, Myhill R and Boffa Ballaran T *et al*. Lower-mantle water reservoir implied by the extreme stability of a hydrous aluminosilicate. *Nature Geosci* 2015; **8**: 75–9.
10. Ohira I, Ohtani E and Sakai T *et al*. Stability of a hydrous δ-phase, $AlOOH$-$MgSiO_2(OH)_2$, and a mechanism for water transport into the base of lower mantle. *Earth Planet Sc Lett* 2014; **401**: 12–7.
11. Lyons TW, Reinhard CT and Planavsky NJ. The rise of oxygen in Earth's early ocean and atmosphere. *Nature* 2014; **506**: 307–15.
12. Evans DAD, Li ZX and Murphy JB. Four-dimensional context of Earth's supercontinents. *Geological Society, London, Special Publications* 2016; **424**: 1–14.
13. Yagi T and Hishinuma T. Iron hydride formed by the reaction of iron, silicate, and water: Implications for the light element of the Earth's core. *Geophys Res Lett* 1995; **22**: 1933–6.
14. Suzuki T, Akimoto S and Fukai Y. The system iron-enstatite-water at high pressures and temperatures—formation of iron hydride and some geophysical implications. *Phys Earth Planet In* 1984; **36**: 135–44.
15. Lavina B and Meng Y. Unraveling the complexity of iron oxides at high pressure and temperature: Synthesis of Fe_5O_6. *Science Advances* 2015; **1**: e1400260.
16. Lavina B, Dera P and Kim E *et al*. Discovery of the recoverable high-pressure iron oxide Fe_4O_5. *Proc Natl Acad Sci U S A* 2011; **108**: 17281–5.
17. Bykova E, Dubrovinsky L and Dubrovinskaia N *et al*. Structural complexity of simple Fe_2O_3 at high pressures and temperatures. *Nat Comms* 2016; **7**: 10661.
18. Lay T, Hernlund J and Buffett BA. Core-mantle boundary heat flow. *Nature Geosci* 2008; **1**: 25–32.
19. Harlov DE and Austrheim H. *Metasomatism and the Chemical Transformation of Rock: The Role of Fluids in Terrestrial and Extraterrestrial Processes*. Berlin: Springer-Verlag, 2013.
20. Frantz JD and Mao HK. Bimetasomatism resulting from intergranular diffusion; II, Prediction of multimineralic zone sequences. *Am J Sci* 1979; **279**: 302–23.
21. Sakamaki K, Takahashi E and Nakajima Y *et al*. Melting phase relation of FeHx up to 20GPa: implication for the temperature of the Earth's core. *Phys Earth Planet In* 2009; **174**: 192–201.
22. Okuchi T. Hydrogen partitioning into molten iron at high pressure: implications for Earth's core. *Science* 1997; **278**: 1781–4.
23. Peacock SA. Fluid processes in subduction zones. *Science* 1990; **248**: 329–37.
24. Williams Q. Water, the solid Earth, and the atmosphere: the genesis and effects of a wet surface on a mostly dry planet. In: Stevenson D (ed.). *Evolution of the Earth*. Amsterdam: Elsevier, 2009, 121–43.
25. van Keken PE, Hacker BR and Syracuse EM. Subduction factory: 4. Depth-dependent flux of H_2O from subducting slabs worldwide. *J Geophys Res: Solid Earth* 2011; **116**: B01401.
26. Dobson DP and Brodholt JP. Subducted banded iron formations as a source of ultralow-velocity zones at the core-mantle boundary. *Nature* 2005; **434**: 371–4.

Downloaded from https://academic.oup.com/nsr/advance-article-abstract/doi/10.1093/nsr/nwx109/4107791
by guest
on 10 December 2017

27. Dziewonski AM and Anderson DL. Preliminary reference earth model. *Phys Earth Planet In* 1981; **25**: 297–356.
28. Birch F. Elasticity and constitution of the Earth's interior. *J Geophys Res* 1952; **57**: 227–86.
29. Frost DJ and Mccammon CA. The redox state of Earth's mantle. *Annu Rev Earth Planet Sci* 2008; **36**: 389–420.
30. Nayar A. Earth science: a lakeful of trouble. *Nature* 2009; **460**: 321–3.
31. Eriksson PG and Condie KC. Cratonic sedimentation regimes in the ca. 2450-2000Ma period: relationship to a possible widespread magmatic slowdown on Earth? *Gondwana Res* 2014; **25**: 30–47.
32. Nance RD, Murphy JB and Santosh M. The supercontinent cycle: a retrospective essay. *Gondwana Res* 2014; **25**: 4–29.
33. Anderson OL, Isaak DG and Yamamoto S. Anharmonicity and the equation of state for gold. *J Appl Phys* 1989; **65**: 1534–43.
34. Wolanin E, Pruzan PH and Chervin JC *et al.* Equation of state of ice VII up to 106 GPa. *Phys Rev B* 1997; **56**: 5781–5.
35. Prakapenka VB, Kubo A and Kuznetsov A *et al.* Advanced flat top laser heating system for high pressure research at GSECARS: application to the melting behavior of germanium. *High Pressure Res* 2008; **28**: 225–35.
36. Meng Y, Hrubiak R and Rod E *et al.* New developments in laser-heated diamond anvil cell with in situ synchrotron x-ray diffraction at High Pressure Collaborative Access Team. *Rev Sci Instrum* 2015; **86**: 072201.
37. Kresse G and Furthmüller J. Efficient iterative schemes for ab initio total-energy calculations using a plane-wave basis set. *Phys Rev B* 1996; **54**: 11169–86.
38. Perdew JP, Chevary JA and Vosko SH *et al.* Atoms, molecules, solids, and surfaces: applications of the generalized gradient approximation for exchange and correlation. *Phys Rev B* 1992; **46**: 6671–87.
39. Perdew JP, Burke K and Ernzerhof M. Generalized gradient approximation made simple. *Phys Rev Lett* 1996; **77**: 3865–8.
40. Dudarev SL, Botton GA and Savrasov SY *et al.* Electron-energy-loss spectra and the structural stability of nickel oxide: an LSDA+U study. *Phys Rev B* 1998; **57**: 1505.
41. Jang BG, Kim DY and Shim JH. Metal-insulator transition and the role of electron correlation in FeO_2. *Phys Rev B* 2017; **95**: 075144.
42. Togo A and Tanaka I. First principles phonon calculations in materials science. *Scripta Mater* 2015; **108**: 1–5.
43. Narygina O, Dubrovinsky LS and Mccammon CA *et al.* X-ray diffraction and Mössbauer spectroscopy study of fcc iron hydride FeH at high pressures and implications for the composition of the Earth's core. *Earth Planet Sc Lett* 2011; **307**: 409–14.
44. Zhu SC, Hu QY and Mao WL *et al.* Hydrogen-bond symmetrization breakdown and dehydrogenation mechanism of FeO2H at high pressure. *J Am Chem Soc* 2017; **139**: 12129–32.

Downloaded from https://academic.oup.com/nsr/advance-article-abstract/doi/10.1093/nsr/nwx109/4107791
by guest
on 10 December 2017
View publication stats